Assessment of non-contacting optical methods to measure wear and surface roughness in ceramic total disc replacements

Green, Naomi C; Bowen, James; Hukins, David Wl; Shepherd, Duncan Et

DOI:
10.1177/0954411915577119

Document Version
Peer reviewed version

Citation for published version (Harvard):
Green, NC, Bowen, J, Hukins, DW & Shepherd, DE 2015, 'Assessment of non-contacting optical methods to measure wear and surface roughness in ceramic total disc replacements', *Institution of Mechanical Engineers. Proceedings. Part H: Journal of Engineering in Medicine*, vol. 229, no. 3, pp. 245-54.
https://doi.org/10.1177/0954411915577119

Assessment of non-contacting optical methods to measure wear and surface roughness in ceramic total disc replacements

Naomi C Green[1], James Bowen[2], David WL Hukins[1], Duncan ET Shepherd[1+]
[1] School of Mechanical Engineering, University of Birmingham, UK

[2] School of Chemical Engineering, University of Birmingham, UK

[+] Corresponding author: Duncan ET Shepherd, University of Birmingham, Edgbaston, B15 2TT, UK
Email d.e.shepherd@bham.ac.uk

Abstract
This study presents a method for measuring the low volumetric wear expected in ceramic Total Disc Replacements (TDRs), which can be used to replace intervertebral discs in the spine, using non-contacting optical methods. Alumina-on-alumina ball-on-disc tests were conducted with test conditions approximating those of cervical (neck region of the spine) TDR wear tests. The samples were then scanned using a three-dimensional non-contacting optical profilometer and the data used to measure surface roughness and develop a method for measuring the wear volume. The results showed that the magnification of the optical lens affected the accuracy of both the surface roughness and wear volume measurements. The method was able to successfully measure wear volumes of 0.0001 mm^3, which corresponds to a mass of 0.0001 mg, which would have been undetectable using the gravimetric method. A further advantage of this method is that with one scan the user can measure changes in surface topography, volumetric wear and the location of the wear on the implant surface. This method could be applied to more severe wear, other types of orthopaedic implants, and different materials.

Keywords
Alumina, Ceramic, Implants, Interferometer, Total Disc Replacement, Wear

1 Introduction

Patients with advanced intervertebral disc degeneration and associated chronic back pain can benefit from having Total Disc Arthroplasty surgery. The affected disc is removed and replaced with a Total Disc Replacement (TDR) device, which is designed to preserve spinal motion.[1] In most TDRs this is achieved with an articulating ball and socket joint, which is formed of two bearing surfaces. Once implanted these bearing surfaces wear, creating submicron sized wear debris which can affect the periprosthetic tissues and cause osteolysis Osteolysis is an inflammatory response to wear debris which eventually leads to aseptic loosening of orthopaedic implants and the need to perform revision surgery.[2-3] Implant

retrieval analyses have shown that aseptic loosening can occur in TDRs with metal-on-metal (M-M) and metal-on-plastic bearings (M-P).[4-7] Whilst there is no published data for ceramic-on-ceramic (C-C) TDRs, studies have shown that osteolysis can occur in ceramic Total Hip Replacement (THR).[8]

It is important to measure the volume of wear debris produced by different TDR bearing materials in order compare their wear performance and their potential to cause osteolysis. *In vitro* wear tests, using spinal simulators, can be used to find volumetric wear rates for TDR devices.[9-10] Although there is no published data for C-C TDRs, retrieval analyses and similar tests on THRs have demonstrated that C-C bearings have low volumetric wear rates. Alumina-on-alumina THRs have been shown to have steady state wear volumes as low as 0.004 $mm^3/10^6$ cycles, which is three orders of magnitude lower than that of M-P bearings.[11]

The standard method for determining the volumetric wear rate of an implant is the gravimetric method, where the change in mass during the test is measured and converted into volume loss. The gravimetric method gives the overall wear volume but not specific data on local wear patterns or the wear mechanism. [12, 13] It is also not suitable for assessing wear of explanted implants as the initial mass is unknown. [12-14] As the design of orthopaedic implants and biomaterials has improved the gravimetric method has reached the limit of its resolution. [14, 15] Indeed some studies of ceramic femoral heads from THRs have concluded that it is practically impossible to measure the volumetric wear rate using the gravimetric method, even with severe wear rates. [11, 12] Therefore given the small size of TDRs and the low wear rate for C-C bearings it will be difficult to accurately measure the mass change due to wear using the gravimetric method. Non-contacting optical measurement methods offer a promising route for determining low wear volumes. They can measure both form and surface roughness in one scan with a vertical resolution of approximately 1 nm and a resolution across the contacting surfaces of approximately 1 μm. Non-contacting optical methods such as white light interferometry[11, 17] and laser confocal profilometry[18] have been successfully used to measure the volumetric wear of ceramic hip and knee implants. They also have the advantage over the gravimetric method that the pattern of wear across the implant surface can be seen and areas of severe wear identified.

The primary objective of this study was to develop a method for measuring the low volumetric wear expected in ceramic TDRs using non-contacting optical methods. A series of alumina-on-alumina, ball-on-disc tests were conducted with test conditions approximating those of cervical TDR wear tests. The test samples were scanned to determine form and surface roughness using a white light interferometer. The data from these scans were then used to develop a method for determining the volume lost during the test due to wear. The study also investigates the effect of changing the magnification of the lens of the interferometer on the surface roughness parameters and volumetric wear calculations.

2 Material and Methods

2.1 Ball-on-Disc Tests

A custom built tribometer (Longshore Systems Engineering, Delabole, UK) was used to carry out ball-on-disc tests (Figure 1a). The ball-on-disc test conditions were based on the International Standards Organisation (ISO) standard for the wear testing of cervical TDRs.[19] The balls were 99.9% purity alumina precision spheres, Grade 50, with a grain size of between 1 and 12 μm (Goodfellow Ceramic and Glass Division, Huntingdon, UK) with the material properties shown in Table 1. The ball had a diameter of 14 mm, chosen to represent the size of a typical cervical TDR (Figure 1b). The discs were 99.7% purity alumina (Dynamic Ceramic, Crewe, UK) with the material properties shown in Table 1. The discs were 20 mm in diameter and 1 mm in thickness (Figure 1b). Before testing, the balls and discs were ultrasonically cleaned in ethanol, wiped with a lint free cloth and left to dry in air at room temperature. The disc was glued (Super Glue Universal, Loctite, Hemel Hempstead, UK) to a glass microscope slide which was then fixed to the rotating base of the tribometer using double sided tape (Nisshin EM Co. Ltd., Tokyo, Japan). The ball was glued (Evo-Stik, Epoxy Rapid, Bostik, Leicester, UK) to a hexagonal M5 cap screw which was then screwed into the lever arm of the tribometer. A normal load of 5 N was applied to the ball, giving a mean Hertzian contact stress of 580 MPa. The disc was rotated against the ball for a distance of 3,665 m. The tests were carried out at sliding velocities of 0.022 m/s and 0.044 m /s, which represent the testing frequencies for the ISO TDR wear tests[19], of 1 Hz and 2 Hz, respectively. To achieve the required velocities the following combinations of disc rotational velocity and radial position of the ball on the disc were used: 3.35 rad/s and 6.5 mm (0.022 m/s); 5.86 rad/s and 7.5 mm (0.044 m/s). The tests were unlubricated, carried out at a controlled room temperature of 18 ± 1°C, and a relative humidity of 30-40%. Each test was repeated four times.

Table 1: Material properties of alumina

	Ball[20]	**Disc[21]**
Alumina Content	99.9%	99.7%
Density (g/cm^3)	3.90	3.89
Young's Modulus (GPa)	365	330
Poisson's Ratio	0.25	0.22
Hardness (GPa)	15.7	15.7

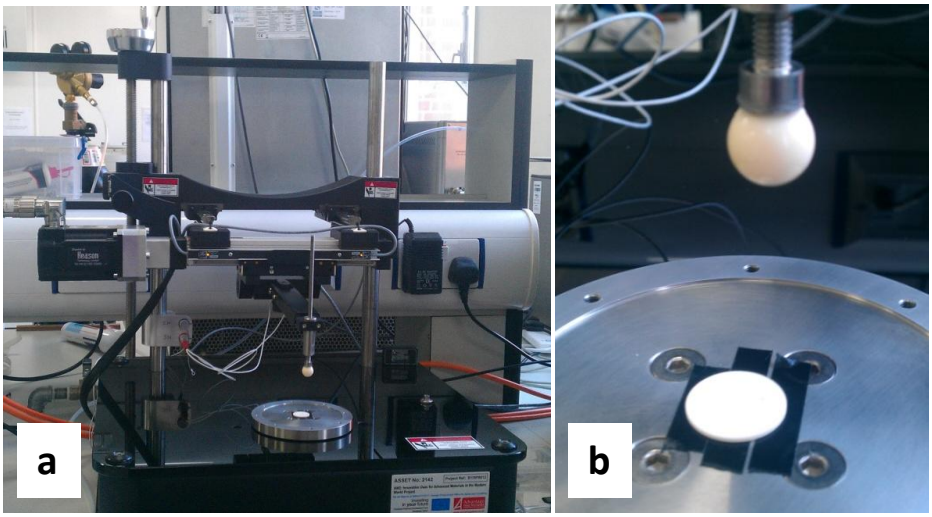

Figure 1: a) Tribometer; b) Alumina ball and disc

2.2 Interferometer

2.2.1 Disc

The surface topography of both the ball and the disc were obtained using a three-dimensional non-contacting optical profilometer, which uses a white light interferometric microscope, MicroXAM2, (KLA Tencor, Wokingham, UK). The data produced by the interferometer was processed and analysed using MapVUE AE version 2.27.1 (KLA Tencor, Wokingham, UK) and Scanning Probe, Image Processor, SPIP version 4.4.3.0 (Image Metrology, Hørsholm, Denmark). The in-plane measurement area, optical resolution, and spatial sampling rate vary depending on the magnification of the microscope, as shown in Table 2. The resolution in the z direction (normal to the x-y plane of the surface of the disc) is approximately 1 nm.

Table 2: Interferometer magnification properties[22]

Objective Magnification	**10×**	**20×**	**50×**
Measurement Area (µm)	827 × 626	413 × 313	165 × 125
Spatial Sampling (µm)	1.1 × 1.3	0.55 × 0.65	0.22 × 0.26
Optical Resolution (µm)	0.92	0.69	0.5

For each disc a section across the wear track was scanned in two different locations with a z depth of 200 µm. In order to scan the full width of the wear track a number of images were stitched together using the stitch function in MapVUE AE. These images were then transferred to SPIP for processing and analysis. The interpolate function was used to fill in void pixels before using the plane correction facility to automatically correct plane distortions in the data using polynomial functions. In this case a first order polynomial was used as the slope on the data appeared linear. The mean z value was then adjusted to zero. To determine the surface roughness before and after the ball-on-disc test a 492 µm × 433 µm area of the main image was sampled in two locations, inside the wear track and on the unworn surface. The surface roughness, S_a, for each location was then calculated using the SPIP software.

2.2.2 Balls

For the balls the wear flat was scanned with a z depth of 400 μm, and a magnification of 10×. The interpolate function was used to fill in void pixels. A region of interest was defined around the observed wear flat on the ball and the rest of the image was excluded from processing. The data inside the region of interest was then corrected for any curvature using the plane correction facility and a second order polynomial. The mean z value was also adjusted to zero. The surface roughness, $S_{a,}$ and dimensions for the wear flat were calculated using the SPIP software. To determine the surface roughness before the ball-on-disc test, a single scan was taken with a z depth of 400 μm, and a magnification of 50×. The image was corrected as above for the wear flat.

2.3 Wear Calculations

2.3.1 Disc

The data from the interferometer was used to calculate the volume loss for the disc. For each of the two interferometer images taken for each disc, an average cross sectional profile of the wear track was calculated using SPIP. The edges of the wear track were found visually and the average profile cut to these edges. The mean surface calculated by the software takes into account the depth of the wear track and is therefore not a true representation of the z depth of the unworn surface. To adjust for this, a new mean surface was calculated from the average of the z depths of the two outer edge data points and subtracted from the z depth values of all the data points. The area above this curve is therefore the cross sectional area of the wear track and was used to calculate the volume loss. Using freeware Octave software, version 3.6.2 (John W Eaton, University Wisconsin Madison, Wisconsin, USA) the approximate cumulative integral of z with respect to x was calculated using trapezoidal integration (Figure 2). The width of the trapezoids is defined by the spatial sampling rate of the interferometer in the x-direction. It was assumed that the calculated cross-sectional area was constant throughout the wear track and therefore the volume loss could be calculated by revolving the area around the circumference of the track.

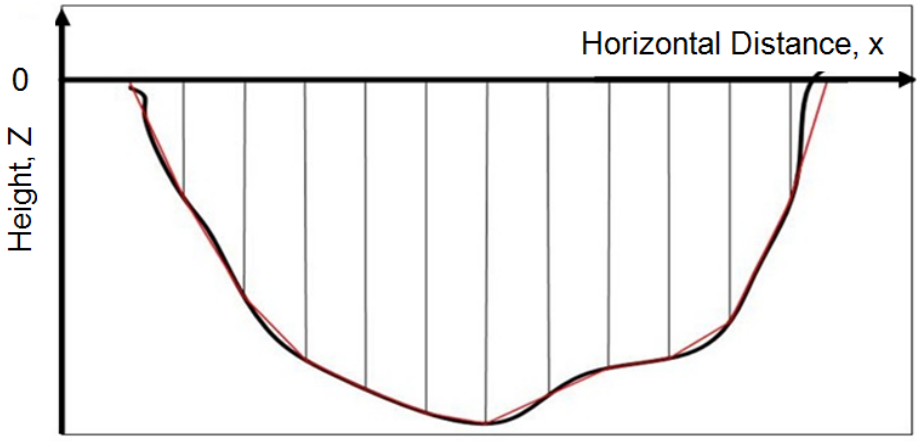

Figure 2: Schematic showing approximate cumulative integral calculated using trapezoidal integration

2.3.2 Balls

For the balls it was assumed that the volume loss, V_b, takes the form of a spherical cap as shown in Figure 3, whose volume was calculated from:

$$V_b = \frac{1}{6}\pi h(3a^2 + h^2) \qquad \text{Equation (1)}$$

where a is the radius of the wear flat and h the height of the spherical cap calculated from:

$$h = r - \sqrt{r^2 - a^2} \qquad \text{Equation (2)}$$

where r is the radius of the ball itself.

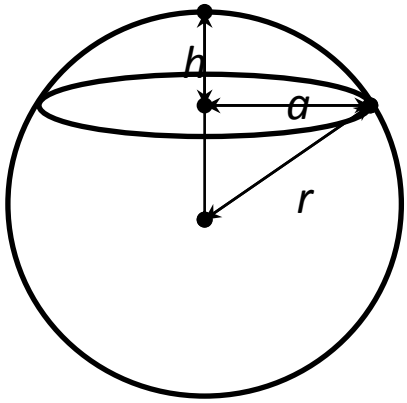

Figure 3: Schematic showing a spherical cap

2.4 Scanning Electron Microscopy

The worn and unworn disc surface topography were sputter-coated with gold and then examined with a Scanning Electron Microscope (SEM), JEOL 7000 (JEOL, Japan) operated at 10.0 kV.

2.5 Statistical Analysis

The statistical analysis was conducted using Minitab version 16.2.3 (Minitab Ltd. Coventry, UK). Anderson-Darling tests were used to check the data followed a normal distribution, based on a probability (p value) of less than 0.05. Two sample t-tests were used to determine if there were significant differences between surface roughness measurements on the worn and unworn surfaces, based on a probability (p value) of less than 0.05.

3 Results

3.1 Surface Study

3.1.1 Disc

The interferometer image of the disc surface, taken with a 10× lens (Figure 4a), clearly shows the loss of material in the wear track and also a small build up of material on the inner edge. The cross sectional profile showing the z depths across the wear track (Figure 4b) clearly supports these observations. Figure 5a shows an image of the same disc, taken with a 20×

lens and the wear track was not so easily identifiable. The cross sectional profile in Figure 5b shows the wear track was positioned higher than the unworn surface which is an incorrect result. This type of image and data were typical of that produced by the 20× lens and suggests a method problem caused by the change in magnification.

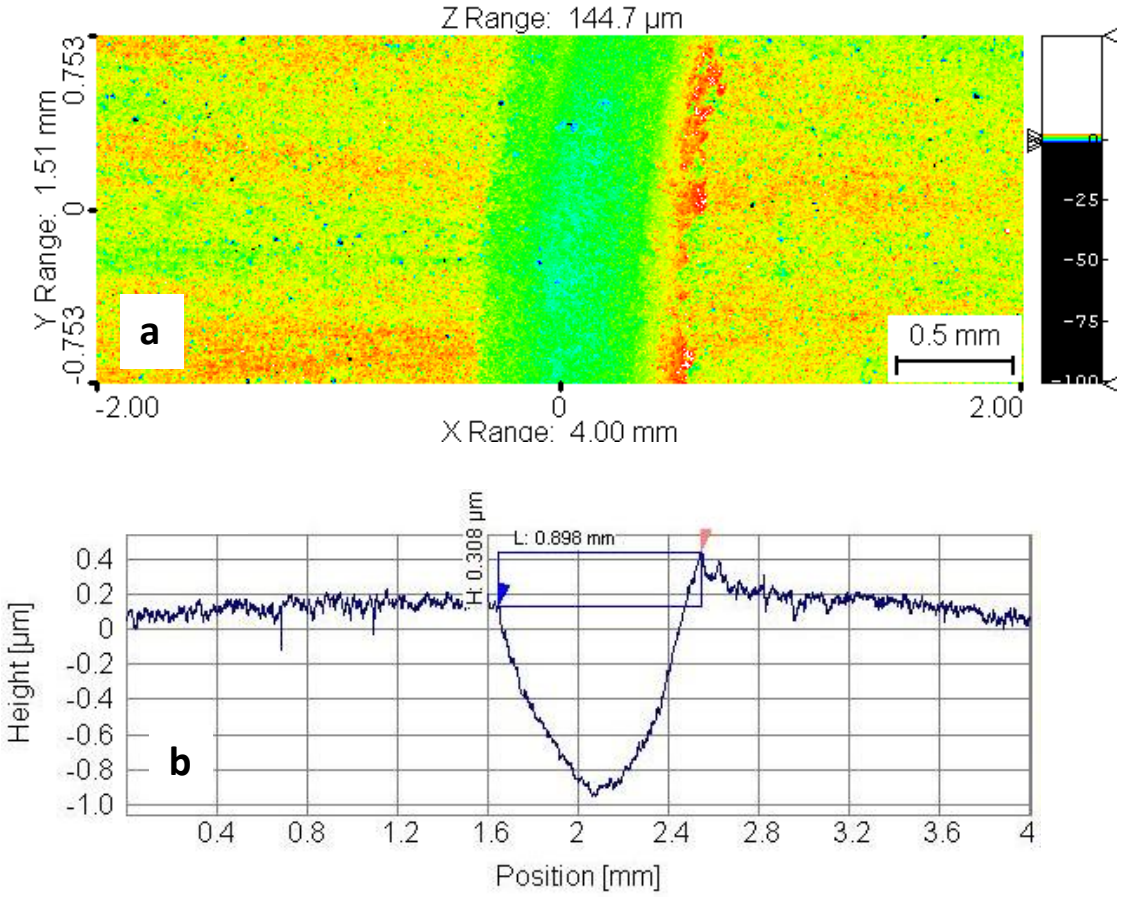

Figure 4: Wear track on an alumina disc after ball-on-disc test conducted at a sliding velocity of 0.022 m/s; a) Interferometer image of z depth taken at 10× magnification; b) Cross sectional profile of the wear track.

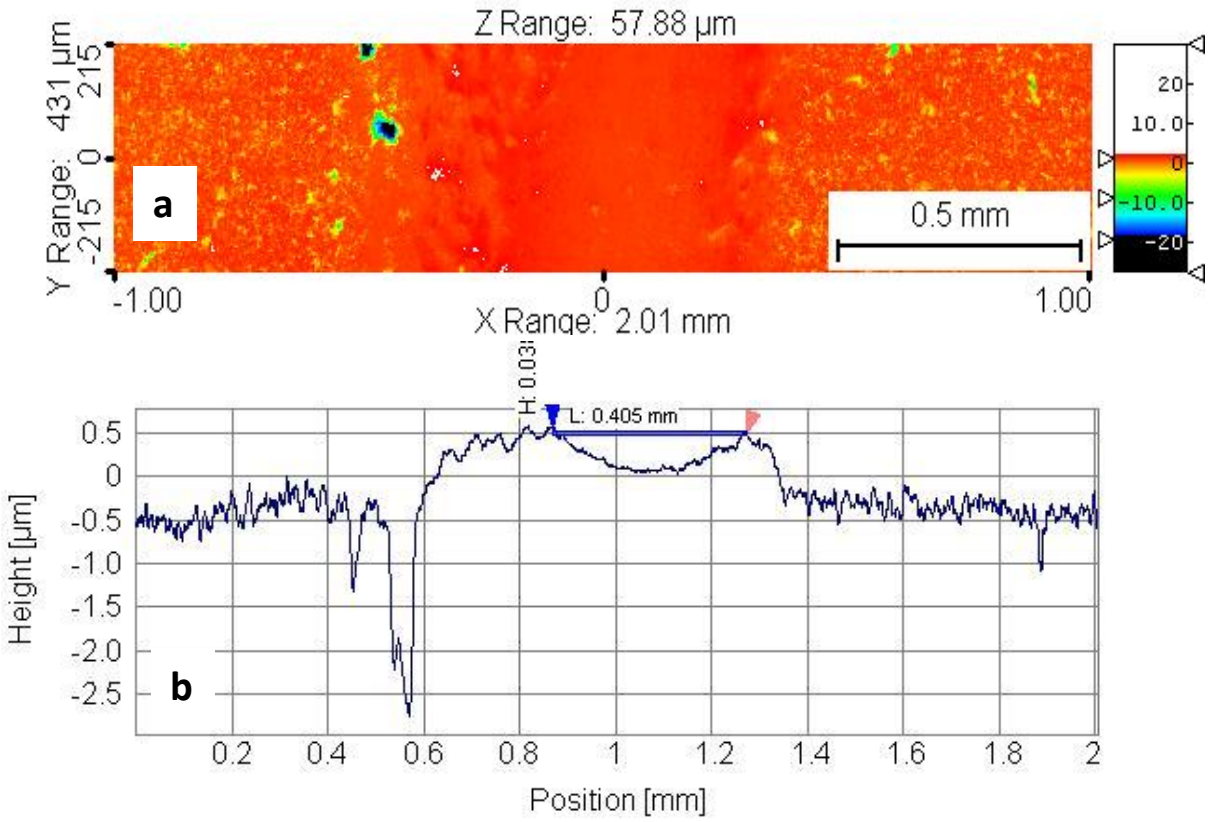

Figure 5: Wear track on an alumina disc after ball on disc test conducted at a sliding velocity of 0.022 m/s; a) Interferometer image of z depth taken at 20× magnification; b) Cross-sectional profile of the wear track.

On visual inspection the worn surface was noticeably more polished than the unworn surface suggesting that the surface roughness was lower on the worn surface. Marks which were left on the discs from the manufacturing process were removed during the test and cannot be seen on the worn surface. There were marks in the direction of travel of the ball in the worn surface suggesting third body wear from wear debris trapped between the ball and the disc.

The surface roughness, S_a, as measured using both a 20× and 10× lens on the interferometer, of the unworn and the worn surfaces is shown in Table 3, with the two measurements for each test denoted by a and b. A two sample t-test showed that the S_a values measured by the 10× and the 20× lens for the unworn surface were significantly different (p=0.000) but there was no significant difference for the worn surface (p=0.313). It was evident from the data that the 20× lens consistently measures a decrease in surface roughness, as seen visually on the surface of the discs. However seven of the 10× lens measurements showed an increase in surface roughness and this was not in agreement with the visual evidence. Therefore, it was assumed that the 20× lens measurements were the more reliable. A two sample t-test on the 20× lens surface roughness measurements confirmed that there was a significant difference between the unworn and worn surfaces (p=0.000).

Table 3: Surface roughness, S_a, interferometer measurements of the unworn and worn disc surface with 10× and 20× lenses

Test No	10× magnification Surface Roughness, S_a (µm)			20× Magnification Surface Roughness, S_a (µm)		
	Unworn Surface	Worn Surface	Change	Unworn Surface	Worn Surface	Change
1a	0.2	0.2	0.0	0.7	0.3	-0.4
1b	0.3	0.2	-0.1	0.8	0.2	-0.5
2a	0.2	0.2	0.0	0.5	0.4	-0.1
2b	0.2	0.2	0.0	0.5	0.4	-0.0
3a	0.2	0.1	-0.1	0.5	0.2	-04
3b	0.2	0.1	-0.1	0.6	0.3	-0.4
4a	0.3	0.2	-0.1	0.7	0.1	-0.5
4b	0.2	0.2	0.0	0.7	0.1	-0.6
5a	0.2	0.3	0.1	0.6	0.3	-0.4
5b	0.2	0.3	0.1	0.6	0.2	-0.4
6a	0.2	0.2	0.0	0.6	0.2	-0.4
6b	0.2	0.2	0.0	0.6	0.2	-0.4
7a	0.8	0.4	-0.4	1.0	0.5	-0.5
7b	0.8	0.4	-0.4	0.8	0.7	-0.1
8a	0.1	0.2	0.0	0.4	0.1	-0.3
8b	0.1	0.2	0.0	0.4	0.1	-0.3
Mean	0.3	0.2	0.0	0.6	0.3	-0.3
Standard Deviation	0.2	0.1	0.2	0.2	0.2	0.2

Visual analysis of the images of all the discs suggested that the 20× lens measures a number of 'pits' in the unworn surface which the 10×lens did not measure. This was confirmed by Figure 6, where one of these pits was imaged with both the 10× and 20× lenses. In Figure 6a the S_a value was 0.683 µm and the maximum depth of the pit was 28 nm and in Figure 6b the S_a value was 0.25 µm and the maximum depth of the pit was 17 nm. These pits were not measured on the worn surface by either the 20× or 10× lenses.

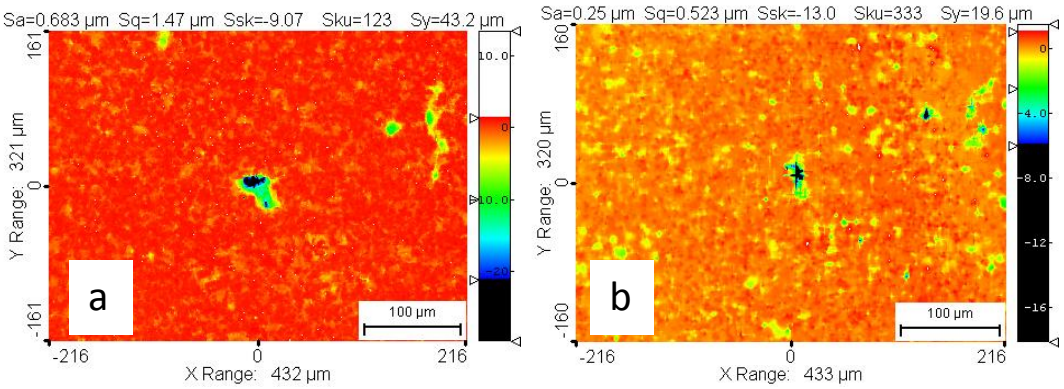

Figure 6: Interferometer image of a pit in the unworn surface of the disc; a) taken with 20× lens; b) taken with 10× lens

Figure 7a shows an SEM image of the surface of the disc shown in Figures 4 and 5. The wear track was clearly identifiable on the image as a dark stripe. The wear track width was measured using the SEM software to be 0.805 mm and compares reasonably well with the interferometer measurement of 0.898 mm from the 10× lens image in Figure 3b. The SEM image agrees with the interferometer images in that there was a series of deep pits on the unworn surface, but they cannot be identified on the worn surface. The detailed SEM image of the worn surface (Figure 7b) showed what appears to be a tribofilm[23] of compacted wear debris and a series of micro-cracks.

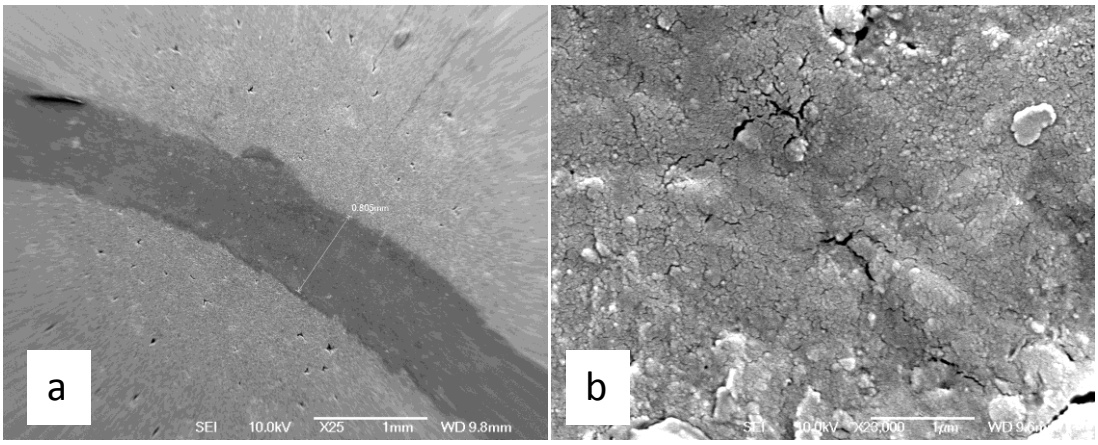

Figure 7: SEM image of an alumina disc after ball-on-disc test conducted at a sliding velocity of 0.022 m/s; a) overview of wear track and unworn surface; b) detailed view of worn surface.

3.1.2 Balls

The three-dimensional interferometer image of a ball, shown in Figure 8a, taken after a ball on disc test, clearly shows the wear flat which formed on the surface during the tests. Figure 8b shows some directional marks, again suggesting third body wear due to trapped wear debris, or possibly a transfer of the tribofilm described above. The surface roughness, S_a, of the unworn and the worn surface of the balls can be seen in Table 4. A two sample t-test showed there was a significant difference between the S_a of the ball before and after the tests (p=0.003). This is supported by the visual appearance of the wear flat being duller than the

unworn surface. The mean S_a of the ball after a 0.044 m/s test was 0.2 ± 0.1 µm and after a 0.022 m/s test was 0.6 ± 0.2 µm.

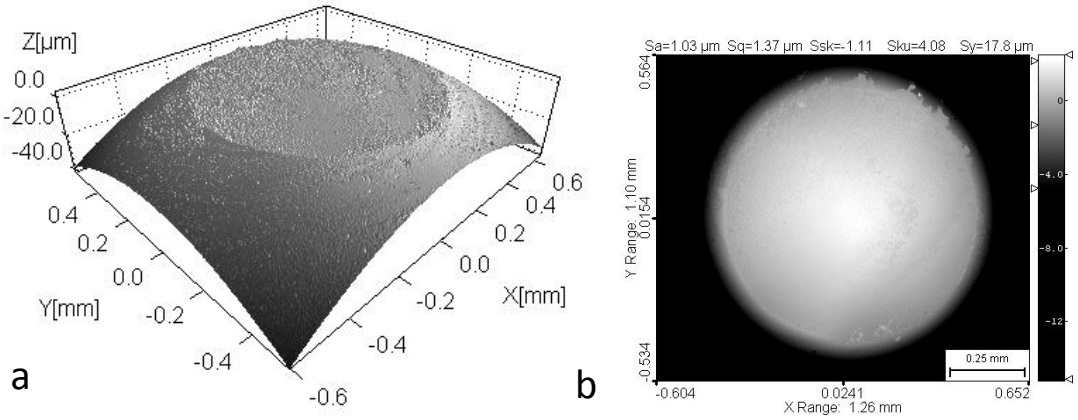

Figure 8: Interferometer image of the wear flat on an alumina ball after ball-on-disc test conducted at a sliding speed of 0.022 m/s; a) three-dimensional image; b) processed two-dimensional image

Table 4: Surface roughness, S_a, interferometer measurements of the unworn and worn ball surfaces (Reported to different precisions due to different measurement techniques)

Test Number	Unworn Surface S_a (µm)	Worn Surface S_a (µm)
1	0.008	0.2
2	0.007	0.1
3	0.014	0.3
4	0.007	0.2
5	0.012	0.6
6	0.008	0.8
7	0.007	0.4
8	0.009	0.7
Mean	0.009	0.4
Standard Deviation	0.003	0.3

3.2 Wear

3.2.1 Discs

The wear volumes for the discs were 0.0194 ± 0.0094 mm^3 (mean ± standard deviation) and 0.0241 ± 0.0133 mm^3 for speeds of 0.044 and 0.022 m/s, respectively. The wear volumes calculated for each disc can be seen in Table 5, with the two measurements for each test denoted by a and b. These wear volumes correspond to a mass loss of 0.0766 ± 0.0368 mg and 0.0950 ± 0.0522 mg, assuming a density value of 3.89 g/cm^3.

Table 5: Disc wear volumes a) velocity 0.044m/s b) velocity 0.022m/s

a)

Test Number	Wear Volume (mm^3)
1a	0.0289
1b	0.0324
2a	0.0223
2b	0.0186
3a	0.0062
3b	0.0067
4a	0.0182
4b	0.0223
Mean	**0.0194**
Standard Deviation	**0.0094**

b)

Test Number	Wear Volume (mm^3)
5a	0.02697
5b	0.0353
6a	0.0263
6b	0.0183
7a	0.0404
7b	0.0345
8a	0.00485
8b	0.0064
Mean	**0.0241**
Standard Deviation	**0.0133**

3.2.2 Balls

The wear volumes for the balls were 0.0015 ± 0.0009 mm^3 (mean ± standard deviation) and 0.0035 ± 0.0026 mm^3 for speeds of 0.044 and 0.022 m/s, respectively (Table 6). These wear volumes correspond to a mass loss of 0.0059 ± 0.0035 mg and 0.0137 ± 0.0101 mg, assuming a density value of 3.90 g/cm^3.

Table 6: Ball wear volumes; a) velocity 0.044m/s; b) velocity 0.022m/s

a)

Test Number	Wear Volume (mm^3)
1	0.0028
2	0.0012
3	0.0008
4	0.0012
Mean	**0.0015**
Standard Deviation	**0.0009**

b)

Test Number	Wear Volume (mm^3)
5	0.0039
6	0.0026
7	0.0067
8	0.0006
Mean	**0.0035**
Standard Deviation	**0.0026**

4 Discussion

The main aim of this study was to develop and assess a novel method for measuring low wear volumes in alumina on alumina TDRs, using non-contacting optical methods. The volume loss due to wear on the discs in these experiments was low and the mass loss would have been in the order of 0.01 mg. The ISO standard for the wear testing of TDRs[19] cites the standard for THRs[24], which specifies the use of a mass balance with an accuracy of ±0.1mg. Such a balance would have been unable to detect the mass loss in these experiments. There

are mass balances on the market which can detect mass changes in the order of 0.0001, 0.001 and 0.01 mg for masses below 2.1, 31 and 60 g respectively.[25, 26] TDR components weigh between 15 and 20 g, but once fixtures which maintain the position of the implant in the wear testing machine are added the combined weight is over 60 g. Analytical balances which can weigh masses above 60 g have a readability of 0.1 mg[26] which would be unable to detect the mass loss in these experiments. Blunt et al[14] have had similar problems with measuring mass changes in the order of 0.005 mg on larger implants, such as THRs and total knee replacements. The method developed in this study can measure volume changes equivalent to a mass loss of 0.0001 mg which is several orders of magnitude lower than suitable mass balances.

Aside from measuring low wear volumes, this non-contacting optical method has the advantage over the gravimetric method that both the form and the surface roughness of the implant can be measured from just one scan. The data can be used to identify changes to the surface topography at the micro-scale and the wear mechanism, and also the location and pattern of the wear at a macro-scale. This method could be further developed to measure the wear in explanted implants, where the initial mass is unknown and the gravimetric method cannot be used.[12-14]

The study also aimed to measure the surface roughness of the worn and unworn surfaces of the test samples and investigate the effect of changing the magnification of the optical lens on the measurements. The worn surfaces of the discs had a mean S_a of 0.3 µm which is significantly lower than the unworn surfaces, which had a mean S_a of 0.6 µm. This can be explained by the presence of a tribofilm covering the wear track and filling in the deep pits in the unworn surface and reducing the surface roughness.[23, 27-32] As the alumina disc wears, grains break away from the surface and are then trapped between the contacting surfaces and ground down into smaller wear particles. The directional marks seen in the disc wear track are indicative of this type of third body wear. Over time these small particles combine together to form agglomerates which are then plastically deformed into compacted layers covering the surface of the wear track. Additional sliding leads to the development of interconnected micro-cracks as seen in the SEM image (Figure 7b).

The presence of this tribofilm has highlighted a potential pitfall with using non-contacting optical methods to measure form. The results show that when using the 20× lens the stitching function gives a spurious result, with the worn surface being higher than the unworn surface. When scanning larger surface areas the interferometer takes a series of smaller scans and then MapVue AE stitches them together to produce one larger scan. The stitching algorithms are designed for surfaces with a reasonably consistent surface roughness. In these tests the 20× lens measured an appreciable difference between the surface roughness of the worn and unworn surfaces. Therefore, there would have been a discontinuity in the surface roughness at the boundary between the worn and unworn surfaces causing the stitching algorithms to misalign the heights of the individual scans. Since the 10× lens does not measure this difference in surface roughness and there is no discontinuity in the scanned surface the

stitching algorithms give more reliable results in terms of form measurement. However, the results also show that the higher resolution of the 20× lens provides more reliable results in terms of surface roughness measurements.

5 Conclusion

A technique for measuring low wear volumes (<0.0001 mm^3/ 0.0001 mg) in ceramic TDRs using non-contacting optical methods was successfully developed. The results showed that this method was able to measure small changes in volume due to wear which would not have been identifiable by using the gravimetric method. The results also showed that, when using non-contacting optical methods, the user needs to be aware of the effect of the magnification of the lens on the reliability of the measurements. This method is not just limited to TDRs and ceramics but could be applied to any orthopaedic implants, made from any material. It would also be useful for measuring more severe wear because the method provides additional information on surface topography and the pattern of the wear on the implant surface. The method could be further developed for use in measuring wear in explanted implants.

Acknowledgments

The Interferometer and Tribometer used in this research were obtained, through Birmingham Science City: Innovative Uses for Advanced Materials in the Modern World (West Midlands Centre for Advanced Materials Project 2), with support from Advantage West Midlands (AWM) and part funded by the European Regional Development Fund (ERDF). N.C. Green is funded by scholarships from the Institution of Mechanical Engineers and the University of Birmingham.

References

[1] Hughes SPF, Freemont AJ, Hukins DWL, et al. The pathogenesis of degeneration of the intervertebral disc and emerging therapies in the management of back pain, J Bone Joint Surg Br 2012; 94B: 1298-1304.

[2] Ingham E, Fisher J. The role of macrophages in osteolysis of total joint replacement. Biomaterials 2005; 26: 1271–1286.

[3] Ingham E, Fisher J. Biological reactions to wear debris in total joint replacement. Proc Inst Mech Eng Part H: J Eng Med 2000; 214: 21-37.

[4] Van Ooij A, Oner FC, Verbout AJ. Complications of artificial disc replacement: a report of 27 patients with the SB Charité disc. J Spinal Disord Tech 2003; 16: 369‑383.

[5] Van Ooij A, Kurtz SM, Stessels F, et al. Polyethylene wear debris and long-term clinical failure of the Charité disc prosthesis: a study of 4 patients. Spine 2007; 32: 223‑229.

[6] Punt IM, Visser VM, Van Rhijn LW, et al. Complications and reoperations of the SB Charité lumbar disc prosthesis: experience in 75 patients. Eur Spine J 2008; 17: 36‑43.

[7] Kurtz SM, Toth JM, Siskey R, et al. The latest lessons learned from retrieval analyses of ultra-high molecular weight polyethylene, metal-on-metal, and alternative bearing total disc replacements. Semin Spine Surg 2012; 24: 57‑70.

[8] Yoon TR, Rowe SM, Jung ST, et al. Osteolysis in association with a total hip arthroplasty with ceramic bearing surfaces J Bone Jt Surg 1998; 80A: 1459-1468.

[9] Xin H, Shepherd DET, Dearn KD, A tribological assessment of a PEEK based self-mating total cervical disc replacement. Wear 2013; 303: 473–479.

[10] Moghadas P, Mahomed A, Hukins DWL, et al Wear in metal-on-metal total disc arthroplasty. Proc Inst Mech Eng Part H: J Eng Med 2004; 227(4): 356–361.

[11] Clarke IC, Good V, Williams P, et al. Ultra-low wear rates for rigid-on-rigid bearings in total hip replacements. Proc Inst Mech Eng Part H: J Eng Med 2000; 214: 214-331.

[12] Sagbas B, Numan Durakbasa M. Measurement of Wear in Orthopaedic Prosthesis. Acta Phys Pol A 2012; 121: 131:134.

[13] Carmignato S, Spinelli M, Affatato S, et al. Uncertainty evaluation of volumetric wear assessment from coordinate measurements of ceramic hip joint prostheses. Wear 2011; 270: 584-590.

[14] Blunt L, Bills P, Jianga X, et al. The role of tribology and metrology in the latest development of bio-materials. Wear 2009; 266: 424-431.

[15] Bills P, Brown L, Jiang X, et al. A metrology solution for the orthopaedic industry. J Phys: Conf Ser 2005; 13: 316-319.

[16] Williams SR, Wu JJ, Unsworth A, et al. Wear and surface analysis of 38 mm ceramic-on-metal total hip replacements under standard and severe wear testing conditions. Proc Inst Mech Eng Part H: J Eng Med 2011; 225: 783-796.

[17] Serra E, Tucci A, Esposito L, et al. Volumetric determination of the wear of ceramics for hip joints. Biomaterials, 2002; 23(4): 1131‑1137.

[18] Turger A, Köhler J, Denkena B, et al. Manufacturing conditioned roughness and wear of biomedical oxide ceramics for all-ceramic knee implants. Biomed Eng Online 2013; 12:84

[19] BS ISO 18192-1:2011 Implants for surgery: Wear of total intervertebral spinal disc prostheses. Part 1: Loading and displacement parameters for wear testing and corresponding environmental conditions for test. British Standards Institute, London 2011.

[20] Ceramic Characteristics Data Sheet received via personal communication from James Taylor, Goodfellows Ceramic and Glass Division, 2nd August 2012.

[21] Dynamic Ceramic, Crewe, UK. Material Properties Retrieved from http://www.dynacer.com/wp-content/themes/devvine/PDF/Material%20Properties%20datasheet.pdf (Accessed 22nd September 2014).

[22] Phase Shift Technology Inc., Arizona, USA. MicroXAM Surface Mapping Microscope. [Brochure] Retrieved from https://cma.tcd.ie/misc/MicroXam.pdf (2002, Accessed 22nd September 2014).

[23] Olofsson J, Bexell U, Jacobson S. Tribofilm formation of lightly loaded self mated alumina contacts. Wear 2012; 289: 39-45.

[24] BS ISO 14242-2:2000 Implants for surgery: Wear of total hip joint prostheses Part 2: Methods of measurement. British Standards Institute, London 2000.

[25] Sartorius UK Ltd. Epsom, UK. Ultramicra and Micro Balances. Retrieved from http://www.sartorius.co.uk/en/products/laboratory/laboratory-balances/ultramicro-micro-balances/ (Accessed 10th December 2014)

[26] Sartorius UK Ltd. Epsom, UK. Analytical Balances. Retrieved from http://www.sartorius.co.uk/en/products/laboratory/laboratory-balances/analytical-balances/ (Accessed 10th December 2014)

[27] Adachi K, Kato K. Formation of smooth wear surfaces on alumina ceramics by embedding and tribo-sintering of fine wear particles. Wear 2000; 245: 84–91.

[28] Singha Roy R, Guchhait H, Chanda A, et al. Improved sliding wear resistance of alumina with sub-micron grain size: A comparison with coarser grained material. J Eur Ceram Soc 2007; 27: 4737-3743.

[29] Adachi K, Kato K, Chen N. Wear map of ceramics. Wear 1997; 203-204: 291-301.

[30] Lee SW, Hsu SM, Munro RG. Ceramic wear maps: SiC whisker reinforced alumina. In Rohatgi PK, Blau PJ, Yust CS (eds) Tribology of composite materials. ASM International, Metals Park. OH. 1990, pp. 35-41.

[31] Kato K, Adachi K. Wear of advanced ceramics. Wear 2002; 253: 1097-1104.

[32] Blomberg A, Olsson M, Hogmark S. Wear mechanisms and tribo mapping of A1203 and Sic in dry sliding. Wear 1994; 171: 77-89.